RESEARCH ARTICLE

A Novel Center-Tapped Rectifier With Current-Balancing and Voltage-Clamped Capability for LLC Resonant Converter

KEON-WOO KIM[1], (Member, IEEE), **MOON-YOUNG KIM**[1], (Member, IEEE),
AND JEONG-IL KANG[2], (Member, IEEE)
[1]Visual Display Business, Samsung Electronics Company Ltd., Suwon-si 16706, Republic of Korea
[2]Digital Appliance Business, Samsung Electronics Company Ltd., Suwon-si 16706, Republic of Korea

Corresponding author: Moon-Young Kim (moon.y.kim@samsung.com)

ABSTRACT A novel center-tapped rectifier with current-balancing and voltage-clamped (CBVC) capability for the LLC resonant converter is proposed. A secondary capacitor is inserted between the contact points of the rectifier diode and the secondary winding of the transformer. The amount of the current flowing through each primary switches and rectifier diodes become almost the same by adopting the CBVC center-tapped rectifier. Equal distribution of the current improves the reliability and lifetime of the primary switches and rectifier diodes. In addition, the voltage across the rectifier diodes in the CBVC center-tapped rectifier is clamped by two times the output voltage. The conduction loss of the rectifier diodes is decreased since the diodes with low forward voltage drop can be used. Moreover, half of the output capacitor is utilized as a secondary side capacitor, which means no additional components. The validity of the proposed converter is verified through experiments on a prototype for 400 VDC input to 45-70 V/4 A output application.

I. INTRODUCTION

There has been a lot of interest in increasing the power density and efficiency. Among many topologies, the LLC resonant converter has been widely used since it can achieve the zero-voltage switching (ZVS), small turn-off losses of the primary switch, and no need for the output filter inductor [1], [2], [3], [4], [5], [6], [7], [8], [9]. In addition, the resonant inductor can be removed by utilizing the leakage inductor of the transformer as the resonant inductor to achieve higher power density. However, small leakage inductance leads to a high ratio of the magnetizing inductance to resonant inductance, which results in low peak voltage gain [3].

In order to obtain both high peak voltage gain and the integrated transformer structure, various works have been studied [10], [11], [12], [13], [14], [15], [16], [17]. A separated bobbin structure is one of the simplest forms to obtain large leakage inductance [10]. Primary and secondary

The associate editor coordinating the review of this manuscript and approving it for publication was Snehal Gawande.

windings are separately wound in different areas, and a low coupling coefficient causes large leakage inductance. In addition, the separated bobbin structure with adjustable leakage inductance is proposed in [11]. This structure changes the leakage inductance by varying the primary and secondary winding structures. However, the winding area cannot be fully used to adjust the leakage inductance. In [12], the leakage inductance is adjusted by changing the core shape. Some areas of the primary winding are not overlapped with the secondary winding resulting in the leakage inductance. However, these core shapes are not commercial items and cannot be universally utilized. To supplement this problem works in [13], [14], and [15] suggest the transformer with controllable leakage inductance using a general EI or UI core. A magnetic shunt structure is considered in [16] and [17], and it increases the leakage inductance by forming an additional magnetic flux path.

The abovementioned studies focus on increasing the primary leakage inductance to remove additional resonant inductors. However, many of these studies also increase the
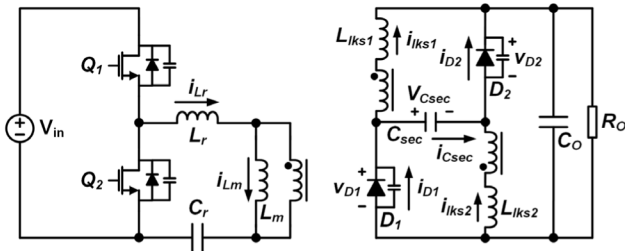
FIGURE 1. Proposed LLC resonant converter with the CBVC center-tapped rectifier.
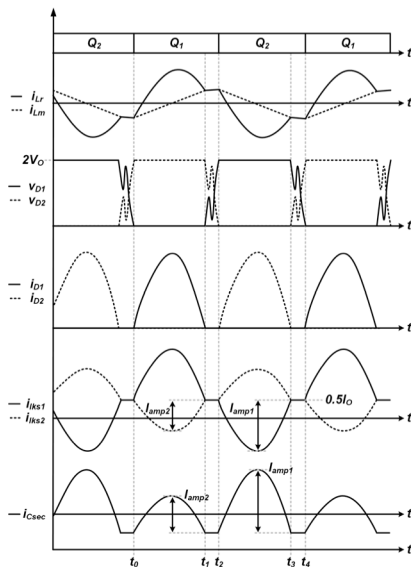
FIGURE 2. Key waveforms of the proposed LLC resonant converter.

FIGURE 3. Current path for each operational modes of the proposed converter. (a) Mode 1. (b) Mode 2. (c) Mode 3. (d) Mode 4.

secondary leakage inductance. Although the work in [18] suggests the magnetic shunt structure with low secondary leakage inductance, the secondary leakage inductance can be increased when the number of turns is increased or the wire-wound transformer is utilized. The secondary leakage inductance leads to undesirable operation for the LLC resonant converter with a center-tapped rectifier, which is widely used for low output voltage applications [19], [20], [21], [22], [23]. First, the voltage stress of the rectifier diodes is increased due to the secondary leakage inductor [19]. High voltage oscillation is occurred because of the resonance between the secondary leakage inductance and junction capacitance of the rectifier diode. In [20], the Taiwan Tech center-tapped rectifier is proposed, and the voltage across the rectifier diodes is clamped to the output voltage. However, this rectifier requires four rectifier diodes which increases the power loss and cost. Also, it is difficult to utilize the SRs due to the necessity of the floating gate driver. Although this rectifier is suitable for high output voltage applications, it has similar performance compared to the full-bridge rectifier in terms of the component count and voltage stress. Second, the difference between the secondary leakage inductances in each winding of the center-tapped rectifier results in the current imbalance problem through the primary side
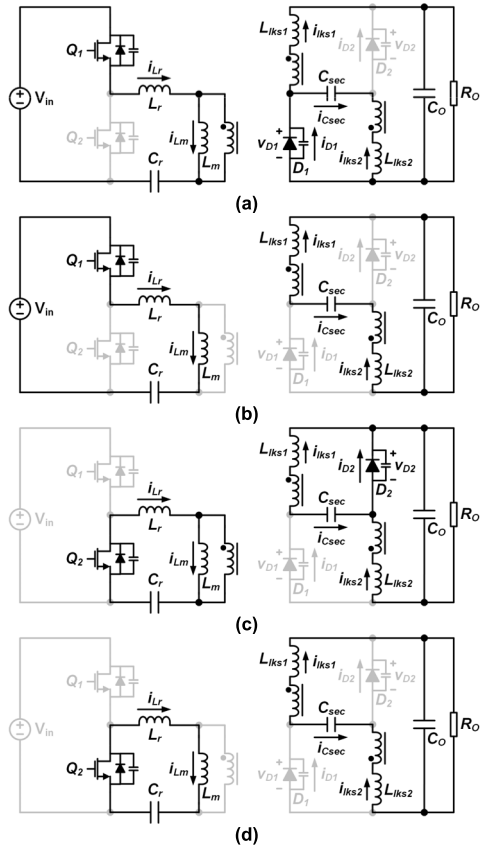
circuit and rectifier diodes [21], [22], [23], [24], [25]. In [21] and [23], the asymmetric duty control on the primary side switches is adopted to balance the current flowing through the rectifiers. However, this control requires current sensing circuit to detect the current imbalance and digital controller to implement another control loop. The asymmetric connection of the transformer is adopted in [25] to reduce the difference between the secondary leakage inductances. Although this method can mitigate the current imbalance problem, two transformers should be utilized which increase the complexity, and it cannot completely equalize the current flowing through rectifier didoes. Current imbalance problem should be solved because it increases the RMS current which causes low efficiency. Also, it leads to unequal loss distribution for primary switches and rectifier diodes which deteriorates the reliability and lifetime of the converter [26], [27].

In this paper, a new center-tapped rectifier with current-balancing and voltage-clamped (CBVC) capability for the LLC resonant converter is proposed, as shown in Fig. 1. In the CBVC center-tapped rectifier, each set of the rectifier diode and secondary winding of the transformer is arranged in an upside-down position. A secondary side capacitor C_{sec} is inserted between the contact points of the rectifier diode and the secondary winding of the transformer. The current balance of primary switches and rectifier diodes is achieved due to the current-balancing loop through C_{sec}.
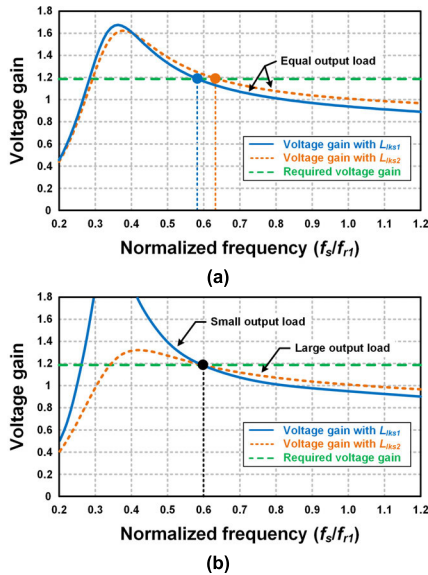
FIGURE 4. Voltage gains of the LLC resonant converter with different secondary leakage inductance. (a) When the current is balanced. (b) When the current is unbalanced.

In addition, the voltage across the rectifier diode is clamped by two times the output voltage regardless of the secondary leakage inductance of the transformer. The current flowing through the output capacitor C_O of the proposed rectifier becomes half compared to that of the conventional center-tapped rectifier, and the other half flows through C_{sec}. Thus, half of C_O can be utilized as C_{sec}. The total volume of C_O and C_{sec} is the same as that of C_O in the conventional center-tapped rectifier. Therefore, the CBVC center-tapped rectifier does not require additional components and enhances the reliability and lifetime of the converter with achieving high efficiency.

The operational principle of the proposed converter is explained in Section II. The voltage gain, current stress of the output capacitor voltage stress of the rectifier diode, and the rectifier circuit configuration for synchronous rectifier are analyzed in Section III. Experimental results to confirm the validity of the proposed converter and the conclusions are given in Sections IV and V, respectively.

II. OPERATIONAL PRINCIPLE OF THE PROPOSED CONVERTER

There are four modes in the proposed converter. The key waveforms and current path for each operational mode during the steady-state are shown in Fig. 2 and 3, respectively. For the simple mode analysis, several assumptions are made as follows:

1) All parasitic components except for those presented in Fig.1 are ignored.

2) Transformer is ideal with its magnetizing inductance L_m and leakage inductances. The primary side leakage inductance L_r is utilized as resonant inductance, and the secondary side leakage inductances are L_{lks1} and L_{lks2}.

3) L_{lks2} is larger than L_{lks1}.

4) C_O and C_{sec} are large enough to be considered as a constant voltage source.

5) The dead time is small enough to be negligible.

The operational principles for each mode are explained as follows:

Mode 1 [$t_0 \sim t_1$]: Mode 1 starts when the primary switch Q_1 is turned on. The current flows through D_1 i_{D1} is divided into C_{sec} and L_{lks1} which are i_{Csec} and i_{lks1}, respectively. During mode1, the amplitude of i_{Csec} is I_{amp2} and identical to that of the current flowing through $L_{lks2}i_{lks2}$. The amplitude of i_{Csec} is smaller than that of i_{lks1} because L_{lks2} is larger than L_{lks1}. The voltage across D_2 v_{D2} is two times the output voltage $2V_O$ since it is the sum of voltages across C_O and C_{sec} which are both V_O.

Mode 2 [$t_1 \sim t_2$]: Mode 2 starts when i_{D1} and the resonant inductor current i_{Lr} become zero and the magnetizing inductor current i_{Lm}, respectively. i_{lks1} and i_{lks2} become the same and maintain the constant value $0.5I_O$ because the voltage across the secondary leakage inductor becomes zero.

Mode 3 [$t_2 \sim t_3$]: Mode 3 starts when the primary switch Q_2 is turned on. The operation is similar to mode 1. The current flows through D_2 i_{D2} is divided into C_{sec} and L_{lks2}. During mode 3, the amplitude of i_{Csec} is I_{amp1} and identical to that of i_{lks1}. Also, i_{lks1} and i_{lks2} are symmetric which means that the amplitudes of i_{lks1} and i_{lks2} during mode 1 and those during mode 3 are the same, respectively. Thus, the amplitude of i_{D2} is the sum of the amplitude of i_{lks1} and i_{lks2} and it is the same with the amplitude of i_{D1}. The voltage across D_1 v_{D1} is $2V_O$ since it is the sum of voltages across C_O and C_{sec} which are both V_O.

Mode 4 [$t_3 \sim t_4$]: Mode 4 starts when i_{D2} and i_{Lr} become zero and i_{Lm}, respectively. The operation is similar to mode 2, and i_{lks1} and i_{lks2} become equal to $0.5I_O$ during mode 4.

III. ANALYSIS OF THE PROPOSED CONVERTER
A. MECHANISM OF CURRENT BALANCE FOR THE PROPOSED CONVERTER

The conventional LLC resonant converter with the center-tapped rectifier has a current imbalance problem through the primary side circuit and rectifier diodes due to the difference of the secondary leakage inductances. The voltage gain of LLC resonant converter can be obtained by the fundamental harmonic approximation [28], and the voltage gains with different secondary leakage inductance according to the normalized frequency are shown in Fig. 4. The normalized frequency is f_s/f_{r1}, and f_s is the switching frequency, $f_{r1} = 1/(2\pi((L_r + n^2L_{lks1})C_r)^{0.5})$, and n is the turns-ratio of the transformer. The voltage gain is different according to the primary switching operation because L_{lks1} is conducted when Q_1 is turned on, and L_{lks2} is conducted when Q_2 is turned on. Assuming that the equal current is flowing through L_{lks1} and L_{lks2}, the switching frequency cannot be the same to regulate required voltage gain, as shown in Fig. 4(a). Thus, the current flowing through the center-tapped
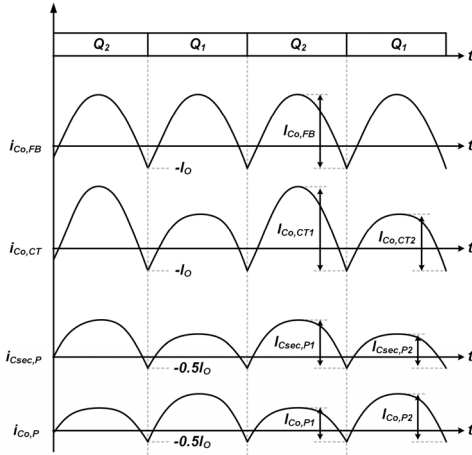
FIGURE 5. Current waveforms flowing through C_O and C_{sec} for the conventional and proposed LLC resonant converter.

FIGURE 6. RMS current of C_O and C_{sec} for the conventional and proposed LLC resonant converter.

rectifier become unbalanced to regulate required voltage gain, as shown in Fig. 4(b).

In the proposed converter, the amplitudes of i_{lks1} and i_{lks2} are different due to the same reason in the conventional center-tapped rectifier. The amplitudes of i_{lks1} during mode 1 and 3 are both I_{amp1}, and the amplitudes of i_{lks2} during mode 1 and 3 are both I_{amp2}. The current flowing through rectifier diodes are equal to the difference between i_{lks1} and i_{lks2}. Thus, the amplitude of i_{D1} and i_{D2} are the same as $I_{amp1} + I_{amp2}$.

B. CURRENT STRESS OF THE OUTPUT CAPACITOR

Normally, the number of C_O for the LLC resonant converter is determined by the RMS current flowing through C_O. Fig. 5 shows the current flowing through C_O and C_{sec} when the converters operate at the resonant frequency. In the LLC resonant converter with the full-bridge rectifier, the amplitude of the current flowing through C_O $I_{Co,FB}$ is the same for each half switching period because the current flows through the same secondary leakage inductor. $I_{Co,FB}$ is $0.5\pi I_O$ since the average current flowing through the rectifier diode is I_O. Then, the RMS current of C_O for the LLC resonant converter with the full-bridge rectifier $I_{Co,FB,RMS}$ is obtained as follows:

$$I_{Co,FB,RMS} = \sqrt{\frac{1}{\pi} \int_0^\pi \left(\frac{\pi}{2} I_O \sin\theta - I_O\right)^2 d\theta}$$
$$= \sqrt{\left(\frac{\pi^2}{8} - 1\right)} I_O. \tag{1}$$

In the LLC resonant converter with the center-tapped rectifier, the amplitudes of the current flowing through C_O for each half switching period $I_{Co,CT1}$ and $I_{Co,CT2}$ are different because of the different secondary leakage inductances. The relationship between $I_{Co,CT1}$ and $I_{Co,CT2}$ is obtained as follows:
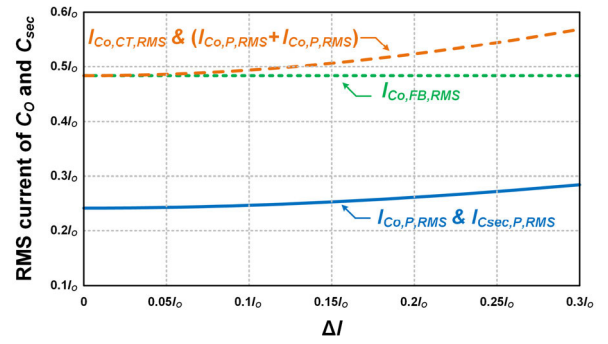
$$I_{Co,CT1} + I_{Co,CT2} = \pi I_O. \tag{2}$$

If the difference between $I_{Co,CT1}$ and $I_{Co,CT2}$ is $2\Delta I$, $I_{Co,CT1} = 0.5\pi I_O + \Delta I$ and $I_{Co,CT2} = 0.5\pi I_O - \Delta I$. The RMS current of C_O for the LLC resonant converter with the center-tapped rectifier $I_{Co,CT,RMS}$ is obtained as follows:

$I_{Co,CT,RMS}$
$$= \sqrt{\frac{1}{2\pi}\left(\int_0^\pi (I_{Co,CT1}\sin\theta - I_O)^2 d\theta + \int_0^\pi (I_{Co,CT2}\sin\theta - I_O)^2 d\theta\right)},$$
$$= \sqrt{\left(\frac{\pi^2}{8}I_O^2 - I_O^2 + \Delta I^2\right)}. \tag{3}$$

In the proposed converter, the ac components of i_{lks1} and i_{lks2} flow through C_O and C_{sec} depending on the switching operation of Q_1 and Q_2. As mentioned earlier, both i_{lks1} and i_{lks2} are symmetrical based on $0.5I_O$. Thus, the amplitudes of the current flowing through C_O when Q_1 is turned on $I_{Co,P1}$ is equal to the amplitudes of the current flowing through C_{sec} when Q_2 is turned on $I_{Csec,P2}$. Also, the amplitudes of the current flowing through C_O when Q_2 is turned on $I_{Co,P2}$ is equal to the amplitudes of the current flowing through C_{sec} when Q_1 is turned on $I_{Csec,P1}$. The relationships between the current flowing through C_O and C_{sec} are obtained as follows:

$$I_{Co,P2} = I_{Csec,P1} = \frac{\pi I_O}{4} + \frac{\Delta I}{2}, \tag{4}$$
$$I_{Co,P1} = I_{Csec,P2} = \frac{\pi I_O}{4} - \frac{\Delta I}{2}, \tag{5}$$
$$I_{Co,P1} + I_{Co,P2} = I_{Csec,P1} + I_{Csec,P2} = \frac{\pi I_O}{2}. \tag{6}$$

The RMS current of C_O and C_{sec} for the proposed converter $I_{Co,P,RMS}$ and $I_{Csec,P,RMS}$ are obtained as follows:

$$I_{Co,P,RMS} = I_{Csec,P,RMS} = \frac{1}{2}\sqrt{\left(\frac{\pi^2}{8}I_O^2 - I_O^2 + \Delta I^2\right)}. \tag{7}$$

Using (1), (3), and (7), the RMS current of C_O and C_{sec} for the conventional and proposed converter is compared in Fig. 6. When ΔI is zero, which means $L_{lks1} = L_{lks2}$, $I_{Co,FB,RMS} = I_{Co,CT,RMS} = I_{Co,P,RMS} + I_{Csec,P,RMS}$, and the number of C_O and C_{sec} are the same for the conventional and proposed converter. According to the increase of ΔI,

TABLE 1. Characteristics of conventional and proposed converters.

	1) LLC with center-tapped rectifier	2) Asymmetric connections of transformers [25]	3) Asymmetric duty control [21,23]	4) Taiwan Tech center-tapped rectifier [20]	5) Proposed converter
Number of rectifier diodes (or SRs)	2	4	2	4	2
Voltage stress of rectifier diodes (or SRs)	$2V_O + \alpha$	$2V_O + \alpha$	$2V_O + \alpha$	V_O	$2V_O$
Current balancing capability	X	△	O	O	O
Synchronous rectifier controller	1 dual-channel SR controller	2 dual-channel SR controller	1 dual-channel SR controller	2 single-channel SR controller + floating gate driver	2 single-channel SR controller
Necessity of current sensing	X	X	O	X	X
Additional components	X	One transformer	X	One capacitor	X

$I_{Co,CT,RMS}$ and $I_{Co,P,RMS} + I_{Csec,P,RMS}$ increase by the same amount. Therefore, the total volume of C_O and C_{sec} in the proposed converter is the same as the volume of C_O in the LLC resonant converter with the center-tapped rectifier.

C. VOLTAGE STRESS OF THE RECTIFIER DIODES

The voltage across the C_{sec} is equal to the voltage across the C_O which is V_O since the voltage across the secondary winding of the transformer is the same as V_O. D_2 acts as a clamping diode when the current flows through D_1, and vice versa. Thus, v_{D1} and v_{D2} are clamped as $2V_O$ when the current is flowing through D_2 and D_1, respectively. During modes 2 and 4 in Section II, the voltages across D_1 and D_2 are determined by the oscillation between the secondary leakage inductances of the transformer and junction capacitances of the rectifier diode. Although the amplitude of the voltage oscillation is varied depending on the parasitic parameters, it does not exceed $2V_O$. Thus, the voltage stress of D_1 and D_2 are $2V_O$.

D. RECTIFIER CIRCUIT CONFIGURATION FOR SYNCHRONOUS RECTIFIER

Synchronous rectifiers (SRs) are widely utilized to replace the rectifier diode, especially in high output current applications. In the conventional center-tapped rectifier, the SRs can be adopted by using a dual-channel SR controller because the source of both SRs is connected to the ground, as shown in Fig. 7 (a). Although one of the SRs in the proposed converter is not connected to the ground, a floating gate driver is not required to drive the SR. The SRs in the proposed converter can be utilized by using two single-channel SR controllers, as shown in Fig. 7 (b). Each SR controller controls the turn-on time by sensing the voltage of the drain and the source of each SR. Also, V_O and voltage across the C_{sec} V_{Csec} are used as the supply voltage for the SR controller 1 and 2, respectively because V_O and V_{Csec} maintain constant voltage based on the source of the SR_1 and SR_2, respectively. Therefore, the rectifier diodes in the proposed converter can be easily replaced by the SRs with two single-channel SR controllers.
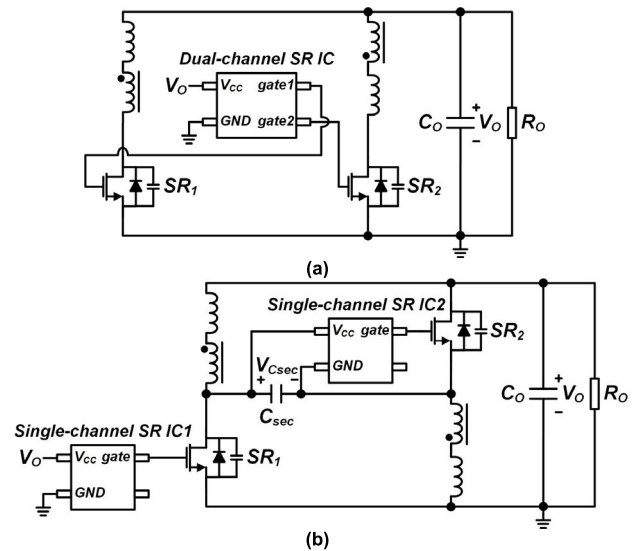

FIGURE 7. Circuit configuration of SR controller. (a) Conventional center-tapped rectifier. (b) CBVC center-tapped rectifier.

E. COMPARISON OF THE CONVENTIONAL AND PROPOSED CONVERTER

The proposed converter is compared with the conventional converters, as shown in Table 1. First, the LLC resonant converter with full-bridge rectifier is composed of 4 rectifier diodes. Although the voltage across the rectifier diodes are clamped by V_O, the conduction loss is increased because the two diodes are conducted for each half switching period. Also, the full-bridge rectifier requires the floating gate driver to utilize the SRs. Second, the LLC resonant converter with center-tapped rectifier has advantages in terms of component count, power loss, and SR implementation. However, the voltage stress of rectifier diodes increases, and current flowing through rectifier diodes is unbalanced due to the leakage inductance of the transformer. The previous research in [19] recommended not to use the separated bobbin to minimize the voltage stress of rectifier diodes. However, the separated bobbin should be used in TV power applications due to
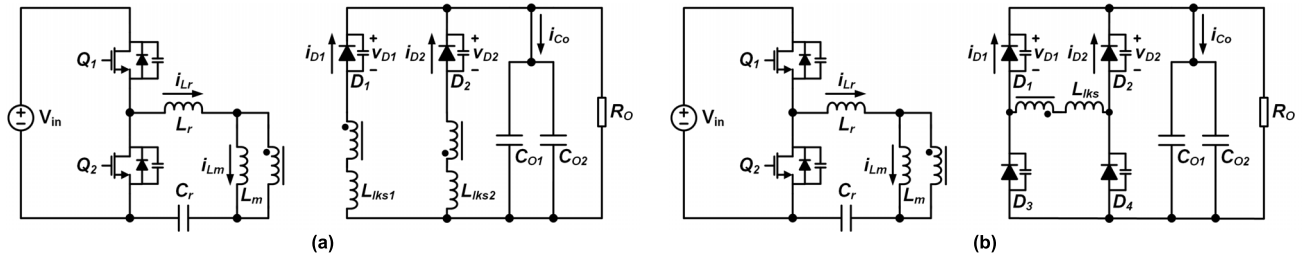
FIGURE 8. Conventional LLC resonant converters. (a) With the center-tapped rectifier. (b) With the full-bridge rectifier.
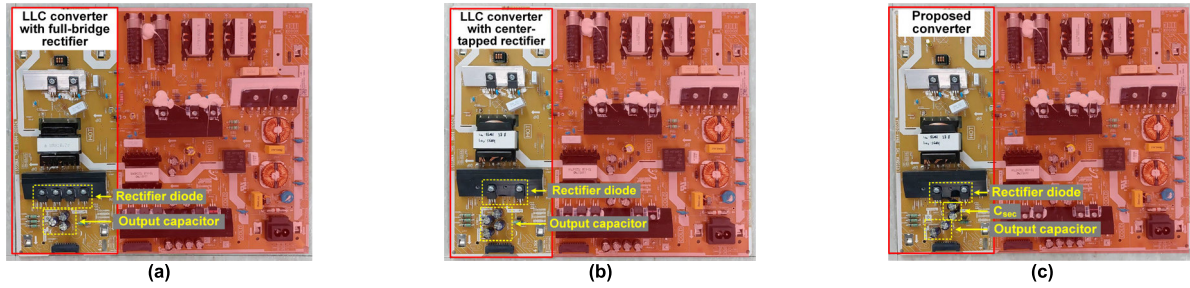

FIGURE 9. Prototype of LLC resonant converters. (a) With the full-bridge rectifier. (b) With the center-tapped rectifier. (c) With the CBVC center-tapped rectifier.

TABLE 2. Component list of prototype converters.

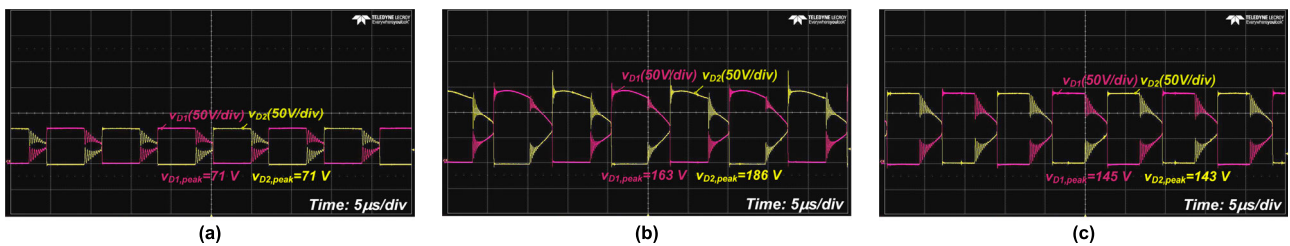|	LLC with full-bridge rectifier	LLC with center-tapped rectifier	Proposed converter
Primary switch	IPP60R125CP (V_{ds}=650 V, I_d=25 A, $R_{ds,on}$=125 mΩ)		
Transformer	EVD4317 (A_e=100.15 mm^2, V_e=5853 mm^3), L_m=560 µH, L_{lkg}=66 µH		
Secondary leakage inductance	L_{lks}=3.2 µH	L_{lks1}=2.6 µH, L_{lks2}=4.7 µH	L_{lks1}=2.6 µH, L_{lks2}=4.7 µH
Resonant capacitor	497B1000V223J (22 nF, 1000 V)		
Rectifier diodes	VF20100C * 4 (V_R=100 V, I_F=20 A)	VS-20CTH03FP (V_R=300 V, I_F=20 A)	VF30200C * 2 (V_R=200 V, I_F=30 A)
Output capacitor	NXQ series capacitor * 3 (100V, 47 µF)	NXQ series capacitor * 4 (100V, 47 µF)	NXQ series capacitor * 2 (100V, 47 µF)
Secondary capacitor	–		NXQ series capacitor * 2 (100V, 47 µF)

FIGURE 10. Waveforms of v_{D1} and v_{D2} (a) With the full-bridge rectifier. (b) With the center-tapped rectifier. (c) With the CBVC center-tapped rectifier.

the insulation standard and minimization of the component count. Third, the converter in [21] uses the asymmetric duty control for the current balancing of the rectifier diodes. However, it suffers from the high voltage oscillation across the rectifier diodes and requires the digital controller to control the primary switches. Fourth, the converter in [20] proposed the Taiwan Tech center-tapped rectifier whose characteristic is similar to the full-bridge rectifier in terms of the component count, voltage stress, and current balancing capability. Its

drawbacks are large number of rectifier diodes, large conduction loss of the rectifier diodes, additional capacitor for rectifier circuit, and requirement of floating gate driver to use SRs. Thus, it is not appropriate for the low-voltage and high-current output applications. Fifth, the converter in [25] utilizes the asymmetric connection of the secondary side windings in the transformer to reduce the current imbalance. There are two secondary side windings due to the center-tapped rectifier structure. The difference of secondary
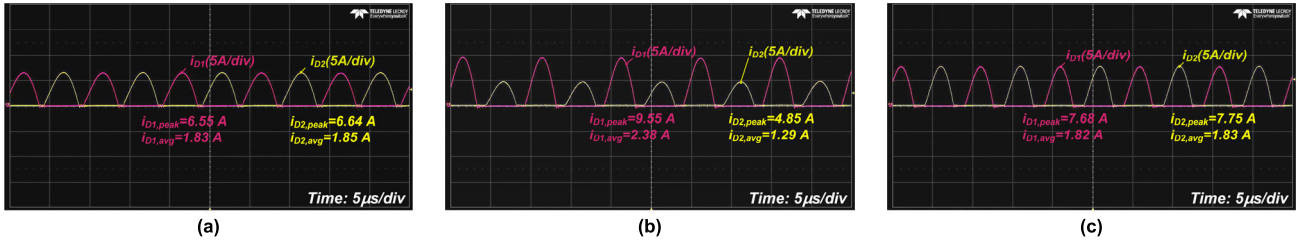
FIGURE 11. Waveforms of i_{D1} and i_{D2} (a) With the full-bridge rectifier. (b) With the center-tapped rectifier. (c) With the CBVC center-tapped rectifier.
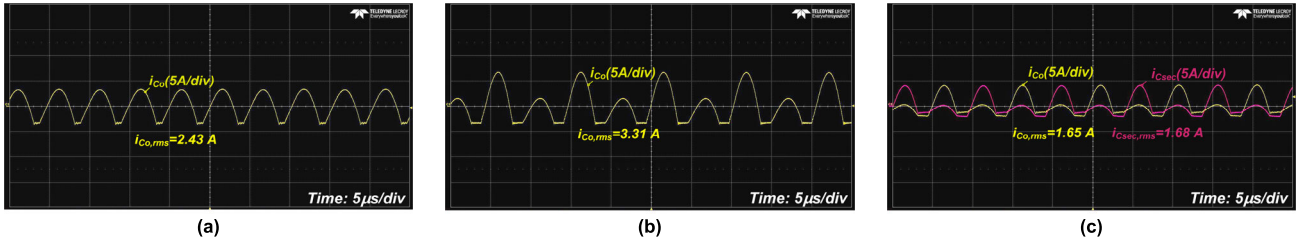

FIGURE 12. Waveforms of i_{Co} and i_{Csec}. (a) With the full-bridge rectifier. (b) With the center-tapped rectifier. (c) With the CBVC center-tapped rectifier.
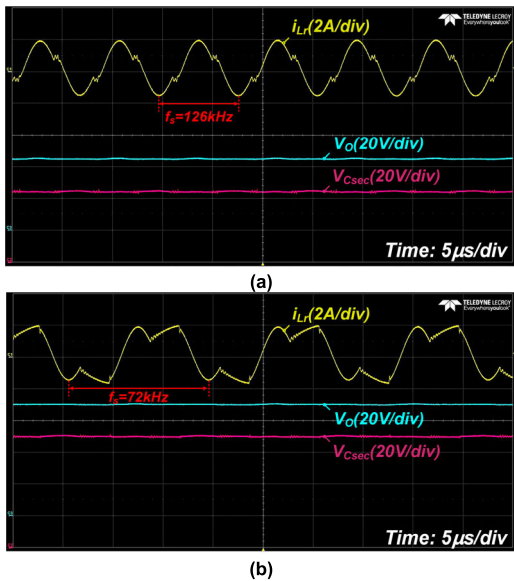

FIGURE 13. Waveforms of i_{Lr}, V_O, and V_{Csec}. (a) When $V_O = 45$ V. (b) When $V_O = 70$V.
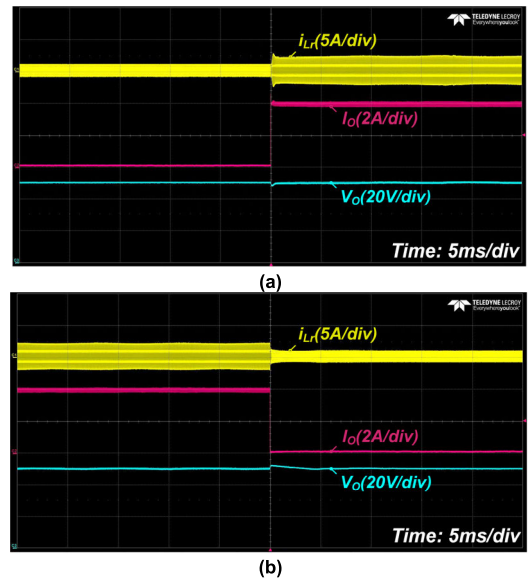

FIGURE 14. Load transient of the proposed converter. (a) When I_O changes from zero to full-load condition. (b) When I_O changes from full to zero-load condition.

side leakage inductances can be decreased by connecting the windings of the two transformers alternately. However, this method cannot fully solve the current imbalance problem and requires two transformers with parallel connection. Finally, in the proposed converter, CBVC center-tapped rectifier is adopted. The voltage stress across the rectifier diodes is clamped by $2V_O$ and the current flowing through the rectifier diodes is balanced. Also, the floating gate driver is unnecessary because V_O and V_{Csec} are utilized for the supply voltage of the SR controllers. In addition, the proposed converter can be composed without additional component and necessity of current sensing. Therefore, the proposed converter is competitive compared to the conventional converters.

IV. EXPERIMENTAL RESULTS

In order to evaluate the performance of the proposed converter, a half-bridge LLC resonant converter is implemented, and the design specifications are as follows: input voltage = 400 V, output = 45-70 V (typ. 50 V)/4 A. Conventional converters are implemented with the half-bridge LLC resonant converter whose secondary side are full-bridge and center-tapped rectifier, as shown in Fig. 8. The prototypes of converters are shown in Fig. 9, and their parameters are listed in Table 2. In the prototype converters, the separated bobbin structure is utilized to obtain large leakage inductance with eliminating additional resonant inductor.
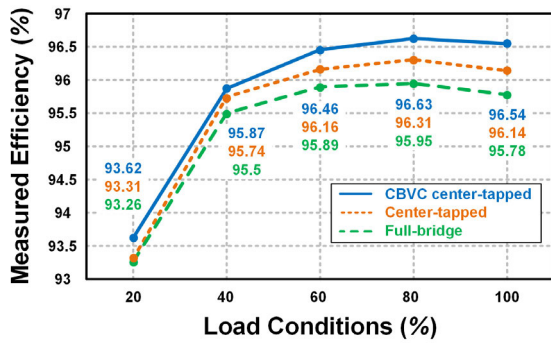
FIGURE 15. Measured efficiency of conventional and proposed converters when V_O = 50 V.
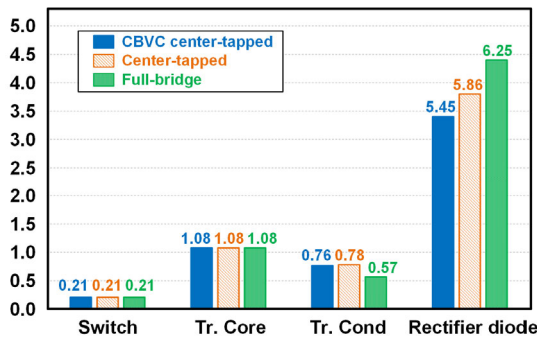

FIGURE 16. Estimated power loss distribution of conventional and proposed converters when V_O = 50 V.

Waveforms of v_{D1} and v_{D2} for the conventional and proposed converters when V_O is the maximum value of 70 V are shown in Fig. 10. v_{D1} and v_{D2} of the full-bridge rectifier are clamped by V_O. However, v_{D1} and v_{D2} of the center-tapped rectifier contain high voltage oscillation since there is no clamping path for the rectifier diodes. In the case of the CBVC center-tapped rectifier, v_{D1} and v_{D2} are clamped by $2V_O$ due to the clamping path through C_{sec}.

Waveforms of i_{D1} and i_{D2} for the conventional and proposed converters when V_O is 50 V are shown in Fig. 11. The amplitude of i_{D1} and i_{D2} are almost the same in the full-bridge rectifier since i_{D1} and i_{D2} flow through the same secondary leakage inductor. However, the amplitudes of i_{D1} and i_{D2} are different in the center-tapped rectifier due to the difference between L_{lks1} and L_{lks2}. The amplitudes of i_{D1} and i_{D2} in the CBVC center-tapped rectifier are almost the same since both are the sum of the amplitude of i_{lks1} and i_{lks2}.

Waveforms of i_{Co} and i_{Csec} under the full load condition for the conventional and proposed converters when V_O is 50 V are shown in Fig. 12. The RMS current of i_{Co} is larger in the center-tapped rectifier compared to the full-bridge rectifier. In the CBVC center-tapped rectifier, the output current is divided into C_O and C_{sec}, and the total RMS current of i_{Co} and i_{Csec} is similar to the RMS current of i_{Co} in the center-tapped rectifier.

The steady state waveforms of i_{Lr}, V_O, and V_{Csec} according to the output voltage are shown in Fig. 13. The switching

frequency changes from 126 to 72 kHz when V_O changes from 45 to 70 V. V_{Csec} maintains the constant value as V_O.

Fig. 14 shows the dynamic response of the proposed converter. Waveforms show V_O when the load changes from zero to the full-load condition and vice versa The proposed converter regulates the output voltage without any undesirable transient under the output load change.

The measured efficiencies and estimated power loss distribution of the conventional and proposed converters according to the load conditions when V_O = 50 V are shown in Fig. 15 and Fig. 16, respectively. In the center-tapped rectifier, the current flows through only one rectifier diode in each half-switching period. However, in the full-bridge rectifier, two rectifier diodes are conducted in each half-switching period. Thus, the LLC resonant converter with the CBVC and conventional center-tapped rectifier have higher efficiency than that with the full-bridge rectifier. Moreover, the LLC resonant converter with the CBVC center-tapped rectifier has higher efficiency than that with the conventional center-tapped rectifier since it can utilize the rectifier diodes with low forward voltage drop.

V. CONCLUSION

A novel center-tapped rectifier with current-balancing and voltage-clamped (CBVC) capability for the LLC resonant converter is proposed. In the CBVC center-tapped rectifier, C_{sec} is inserted between the contact points of the rectifier diode and the secondary winding of the transformer. C_{sec} has two functions: 1) Equalizing the current flowing through rectifier diodes. 2) Clamping the voltage across the rectifier diodes by $2V_O$. In addition, an additional capacitor is not required for C_{sec} since half of the output capacitor can be utilized as C_{sec}. In this paper, the operational principle of the proposed converter is explained. The voltage gain, current stress of the output capacitor, and the voltage stress of the rectifier diodes are analyzed. The validity of the proposed converter is verified by comparing the proposed converter and the LLC resonant converters with the full-bridge and center-tapped rectifier. The current-balancing and voltage-clamping characteristics of the CBVC center-tapped rectifier are experimentally verified. Moreover, the proposed converter has a higher efficiency than the conventional converters under the entire load conditions due to the smaller conduction loss of the rectifier diodes. In conclusion, the proposed converter increases the efficiency and improves the reliability and lifetime of the LLC resonant converter, especially with the large secondary leakage inductance such as the converter using the separated bobbin or low-profile transformer.

REFERENCES

[1] M. A. Saket, N. Shafiei, and M. Ordonez, "LLC converters with planar transformers: Issues and mitigation," *IEEE Trans. Power Electron.*, vol. 32, no. 6, pp. 4524–4542, Jun. 2017.

[2] J.-W. Kim and G.-W. Moon, "A new LLC series resonant converter with a narrow switching frequency variation and reduced conduction losses," *IEEE Trans. Power Electron.*, vol. 29, no. 8, pp. 4278–4287, Aug. 2014.

[3] Y. Jeong, M.-S. Lee, J.-D. Park, J.-K. Kim, and R. A. L. Rorrer, "Hold-up time compensation circuit of half-bridge LLC resonant converter for high light-load efficiency," *IEEE Trans. Power Electron.*, vol. 35, no. 12, pp. 13126–13135, Dec. 2020.

[4] M. G. L. Roes, J. L. Duarte, and M. A. M. Hendrix, "Disturbance observer-based control of a dual-output LLC converter for solid-state lighting applications," *IEEE Trans. Power Electron.*, vol. 26, no. 7, pp. 2018–2027, Jul. 2011.

[5] K.-W. Kim, H.-S. Youn, J.-I. Baek, Y. Jeong, and G.-W. Moon, "Analysis on synchronous rectifier control to improve regulation capability of high-frequency LLC resonant converter," *IEEE Trans. Power Electron.*, vol. 33, no. 8, pp. 7252–7259, Aug. 2018.

[6] K.-W. Kim, Y. Jeong, J.-S. Kim, and G.-W. Moon, "Low common-mode noise LLC resonant converter with static-point-connected transformer," *IEEE Trans. Power Electron.*, vol. 36, no. 1, pp. 401–408, Jan. 2021.

[7] Y. Wei, Q. Luo, X. Du, N. Altin, A. Nasiri, and J. M. Alonso, "A dual half-bridge LLC resonant converter with magnetic control for battery charger application," *IEEE Trans. Power Electron.*, vol. 35, no. 2, pp. 2196–2207, Feb. 2020.

[8] J.-W. Kim, M.-H. Park, B.-H. Lee, and J.-S. Lai, "Analysis and design of LLC converter considering output voltage regulation under no-load condition," *IEEE Trans. Power Electron.*, vol. 35, no. 1, pp. 522–534, Jan. 2020.

[9] S. Moon, C. Chen, and R.-J. Wang, "A new dead time regulation synchronous rectification control method for high efficiency LLC resonant converters," *IEEE Trans. Power Electron.*, vol. 36, no. 9, pp. 10673–10683, Sep. 2021.

[10] S. De Simone, C. Adragna, and C. Spini, "Design guideline for magnetic integration in LLC resonant converters," in *Proc. Int. Symp. Power Electron., Electr. Drives, Autom. Motion*, Jun. 2008, pp. 950–957.

[11] S. Rahman, V. Sidorov, A. Chub, and D. Vinnikov, "High-frequency split-bobbin transformer design with adjustable leakage inductance," in *Proc. IEEE 62nd Int. Scientific Conf. Power Electr. Eng. Riga Tech. Univ. (RTUCON)*, Nov. 2021, pp. 1–5.

[12] M. H. Ahmed, A. Nabih, F. C. Lee, and Q. Li, "Low-loss integrated inductor and transformer structure and application in regulated LLC converter for 48-V bus converter," *IEEE J. Emerg. Sel. Topics Power Electron.*, vol. 8, no. 1, pp. 589–600, Mar. 2020.

[13] B. Li, Q. Li, and F. C. Lee, "High-frequency PCB winding transformer with integrated inductors for a bi-directional resonant converter," *IEEE Trans. Power Electron.*, vol. 34, no. 7, pp. 6123–6135, Jul. 2019.

[14] M. D'Antonio, S. Chakraborty, and A. Khaligh, "Planar transformer with asymmetric integrated leakage inductance using horizontal air gap," *IEEE Trans. Power Electron.*, vol. 36, no. 12, pp. 14014–14028, Dec. 2021.

[15] X. Chen, G. Xu, Q. Shen, Y. Sun, and M. Su, "Magnetizing and leakage inductance integration for split transformers with standard UI cores," *IEEE Trans. Power Electron.*, vol. 37, no. 11, pp. 12980–12985, Nov. 2022.

[16] M. Li, Z. Ouyang, and M. A. E. Andersen, "High-frequency LLC resonant converter with magnetic shunt integrated planar transformer," *IEEE Trans. Power Electron.*, vol. 34, no. 3, pp. 2405–2415, Mar. 2019.

[17] S. Arab Ansari, J. N. Davidson, and M. P. Foster, "Fully-integrated planar transformer with a segmental shunt for LLC resonant converters," *IEEE Trans. Ind. Electron.*, vol. 69, no. 9, pp. 9145–9154, Sep. 2022.

[18] S. A. Ansari, J. N. Davidson, and M. P. Foster, "Inserted-shunt integrated planar transformer with low secondary leakage inductance for LLC resonant converters," *IEEE Trans. Ind. Electron.*, vol. 70, no. 3, pp. 2652–2661, Mar. 2023.

[19] K.-B. Park, B.-H. Lee, G.-W. Moon, and M.-J. Youn, "Analysis on center-tap rectifier voltage oscillation of LLC resonant converter," *IEEE Trans. Power Electron.*, vol. 27, no. 6, pp. 2684–2689, Jun. 2012.

[20] C.-S. Leu, P.-Y. Huang, and W.-K. Wang, "LLC converter with Taiwan tech center-tapped rectifier (LLC-TCT) for solar power conversion applications," in *Proc. 1st Int. Future Energy Electron. Conf. (IFEEC)*, Nov. 2013, pp. 515–519.

[21] C.-O. Yeon, D. K. Kim, J.-B. Lee, J.-W. Kim, C.-Y. Lim, and G.-W. Moon, "Digital implementation of optimal SR ON-time control and asymmetric duty control in LLC resonant converter," in *Proc. 9th Int. Conf. Power Electron. ECCE Asia (ICPE-ECCE Asia)*, Jun. 2015, pp. 2031–2037.

[22] J.-H. Jung, "Bifilar winding of a center-tapped transformer including integrated resonant inductance for LLC resonant converters," *IEEE Trans. Power Electron.*, vol. 28, no. 2, pp. 615–620, Feb. 2013.

[23] M. Li, Q. Chen, X. Ren, Y. Zhang, K. Jin, and B. Chen, "The integrated LLC resonant converter using center-tapped transformer for on-board EV charger," in *Proc. IEEE Energy Convers. Congr. Expo. (ECCE)*, Sep. 2015, pp. 6293–6298.

[24] M. Sato, S. Nagaoka, T. Uematsu, and T. Zaitsu, "Mechanism of current imbalance in LLC resonant converter with center tapped transformer," in *Proc. Int. Power Electron. Conf. (IPEC-Niigata-ECCE Asia)*, May 2018, pp. 118–122.

[25] I. Demirel and B. Erkmen, "A very low-profile dual output LLC resonant converter for LCD/LED TV applications," *IEEE Trans. Power Electron.*, vol. 29, no. 7, pp. 3514–3524, Jul. 2014.

[26] J. Kucka and D. Dujic, "Equal loss distribution in duty-cycle controlled H-bridge LLC resonant converters," *IEEE Trans. Power Electron.*, vol. 36, no. 5, pp. 4937–4941, May 2021.

[27] M. R. Chowdhury, S. Chowdhury, M. A. Rahman, M. R. Islam, M. A. P. Mahmud, and A. Z. Kouzani, "Model predictive control based advanced switching strategy for H-bridge converter used in SMES applications to obtain even loss sharing," *IEEE Trans. Appl. Supercond.*, vol. 31, no. 8, pp. 1–6, Nov. 2021.

[28] R. L. Steigerwald, "A comparison of half-bridge resonant converter topologies," *IEEE Trans. Power Electron.*, vol. 3, no. 2, pp. 174–182, Apr. 1988.

KEON-WOO KIM (Member, IEEE) received the B.S., M.S., and Ph.D. degrees in electrical engineering from the Korea Advanced Institute of Science and Technology (KAIST), Daejeon, South Korea, in 2015, 2017, and 2021, respectively. In 2021, he joined the Visual Display, Samsung Electronics Company Ltd., Suwon-si, South Korea, and began working on the power system for various display. His main research interests include high efficiency and slim profile power converters, the control of power converters, and low EMI noise converters.

MOON-YOUNG KIM (Member, IEEE) was born in South Korea, in 1982. He received the B.S. degree from Kyung-Pook National University (KNU), Daegu, South Korea, in 2008, and the M.S. and Ph.D. degrees in electrical engineering from the Korea Advanced Institute of Science and Technology (KAIST), Daejeon, in 2010 and 2014, respectively.

He is currently a Principle Engineer with Samsung Electronics, Suwon-si, South Korea. His main research interests include the design and control of a DC/DC converter and the power system of display. He is a member of the Korean Institute of Power Electronics (KIPE).

JEONG-IL KANG (Member, IEEE) received the B.S., M.S., and Ph.D. degrees in electrical engineering from the Korea Advanced Institute of Science and Technology (KAIST), Daejeon, South Korea, in 1995, 1997, and 2002, respectively. He joined the Visual Display Business for Samsung Electronics Company Ltd., Suwon-si, South Korea, and started his job in power system development for various products including TV, monitor, projector, and sound bar. In 2023, he was moved to the Digital Appliance Business for the same company to start his new career with power systems for various appliances, including refrigerator, washer, air conditioner, cooker, and cleaner. Since 2018, he has been a Master (Research VP) of Samsung in the area of power electronics. He is currently in charge of the Power Electronics Laboratory as the Head of Lab. His main research interests include AC/DC converters, DC/DC converters, DC/AC inverters, LED drivers, and eco-friendly power systems. He is a member of the Korean Institute of Power Electronics (KIPE).

• • •